Mon. Not. R. Astron. Soc. **000**, 000–000 (0000) Printed 20 February 2013 (MN LaTeX style file v2.2)

Effects of bulk gas rotation on the emergent Lyman-α line in distant galaxies

Nicolas Garavito.[1] Jaime E. Forero-Romero[2]

[1] *Uni A* [2] *Uni B*

20 February 2013

ABSTRACT

Key words: galaxies: high-redshift - galaxies: star formation - line: formation

1 INTRODUCTION

Due to the resonant nature of the lyman alpha line, gas kinematics play an important role in the shape of this line. In particular we study the case in which this gas is spherically symmetric and its rotating.

2 IMPLEMENTATION OF BULK GAS ROTATION

We implement into CLARA the simplest model whereby a sphere rotates with homogeneous angular velocity. We define a cartesian coordinate system with its origin at the center of the sphere and the rotation axis to be the z-axis, the components in the bulk velocity field, $\vec{v} = v_x\hat{i} + v_y\hat{j} + v_z\hat{z}$. in the gas can be written as

$$v_x = -\frac{y}{R}V_{\max}, \quad (1a)$$

$$v_y = \frac{x}{R}V_{\max}, \quad (1b)$$

$$v_z = 0, \quad (1c)$$

where R is the radius of the sphere and $V_{\max}$ is the linear velocity at the sphere's surface. The minus sign in the x-component of the velocity is due to the direction of rotation, in this case we assume that the angular velocity vector goes in the $\hat{k}$ direction.

3 GRID OF SIMULATED MODELS

We compute the emergent Lyman-α line for several models with differents values for the maximal rotational velocity, hydrogend optical depth, dust optical depth and initial distributions of the photons with respect to the gas. There are in total 60 models with the input parameters summarized in Table 1.

Additionaly in the postprocessing process we will take into account different observer positions with respecto the cloud rotation axis.

Now if we take into account the position of the observer and compute this for differents angles of observation θ the outcoming spectra is modified as is shown in figure[2]. The main feature here is that as the angle increases the line high decreases. It means that a observer in the poles will observe a higher double peak than a observer in the ecuator. We will understand this in more details when we present the resaults of the scape fraction in section[].

Velocity (km s^{-1})	$V_{\max}$	$0,\ 50,\ 100,\ 200,\ 300$
Hydrogen Optical Depth	τ_H	$10^5,\ 10^6,\ 10^7$
Dust Optical Depth	τ_A	XXX
Photons Distributions		Central, Homogeneous

Table 1. Values for the varying input parameters in CLARA. Taking into account all the possible combinations for these models

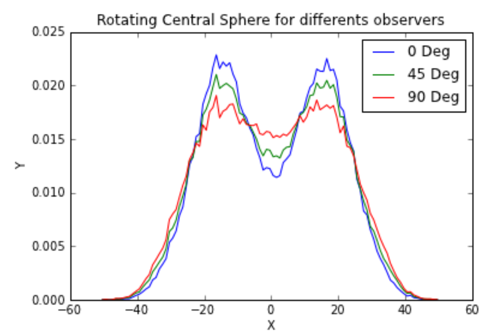

Figure 2. Spectra for different observers. Model:$V = 300km/s$, Optical Depth $\tau = 10^7$ and Central Distribution without dust.

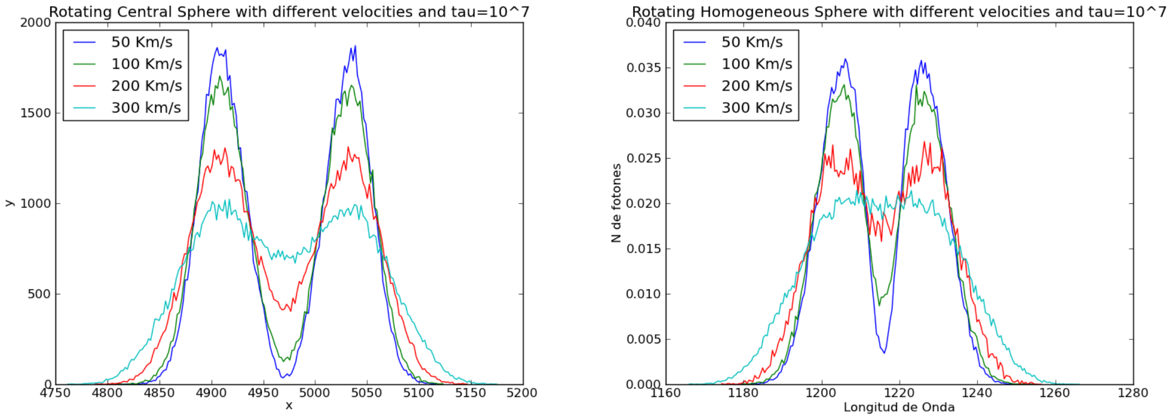

Figure 1. Shape of the lyman alpha line for differents velocities. The left panel show the central distribution while the right panel show the homogeneous distribution.

4 RESULTS

In the previous section we describe the models that we study the effect of rotation in the Lyman alpha line and see the effect of rotation in the specrtums. Now we show the main resaults that we obtain, in particual we pay spetial attention to the position of the maximums, the width of the line and the escape fraction in function of the rotational velocity and the angle of observation θ.

In Figure[1] the effect that rotation have in the spectra is shown, for both distributions central (Left) and homogeneous (right). This is a general case in the sense that is independent of the position of an external observer.

4.1 Maximums Position

(comparar con la grafica del apendice de clara con el eje x el optical depth y en el eje-y los maximos)

The maximus position gives information about the wave lenght of the mayority of the outcoming photons after they interact with the gas, in addition as a photon have more scatterings its wave lenght would be larger than the initial which is 1216 Å. As we can see in Fig.[3] the position of the maximums does not change with rotational velocity. But it change from homogeneous and central.

4.2 Line Width

Another effect that the rotation of the gas produce is in the width of the lyman alpha line. The width of the line provide information of the the how many phtons scape with a particular wave lenght, in the ideal case in which all the photons scape with the same wave lenght the outcoming spectrum would be narrow. For all the models we study we found that as the rotational velocity increase as the line width increase this is show in Fig.[4].

We also found that the width for a particular model is not the same for differents angles of observation in particular as the angle increase the width also increase, it means that as the angle increase the number of scatterings of the photons increasse for this reason we see a broader line. Fig.[5]

Velocity (Km/s)	Maximum 1 position	Maximum 2 position
50	-16.2695	16.23705
100	-15.66496	15.33504
200	-16.93149	14.56851
300	-13.40048	16.09952

Table 2. Optical Depth $\tau = 10^7$, Central Distribution

4.3 Escape Fraction

The fraction of photons that escape from de cloud of gas and dust is defined as:

$$F_e = \frac{\Sigma_{NI}\vec{k}\cdot\vec{o}}{\Sigma_{NF}\vec{k}\cdot\vec{o}} \tag{2}$$

Where NI is the initial number of photons and NF is the final. This escape fraction is computed for all the models which resaults are shown in Fig.[6]

When the distribution is homogeneous the effect of velocity in the escape fraction is clear while in the central model the effect is not noterous. The main effect is that the escape fraction increase as the velocity increase.

5 DISCUSSION

6 OBSERVATIONAL IMPLICATIONS

7 CONCLUSIONS

ACKNOWLEDGEMENTS

APPENDIX A: TABLES

Line width

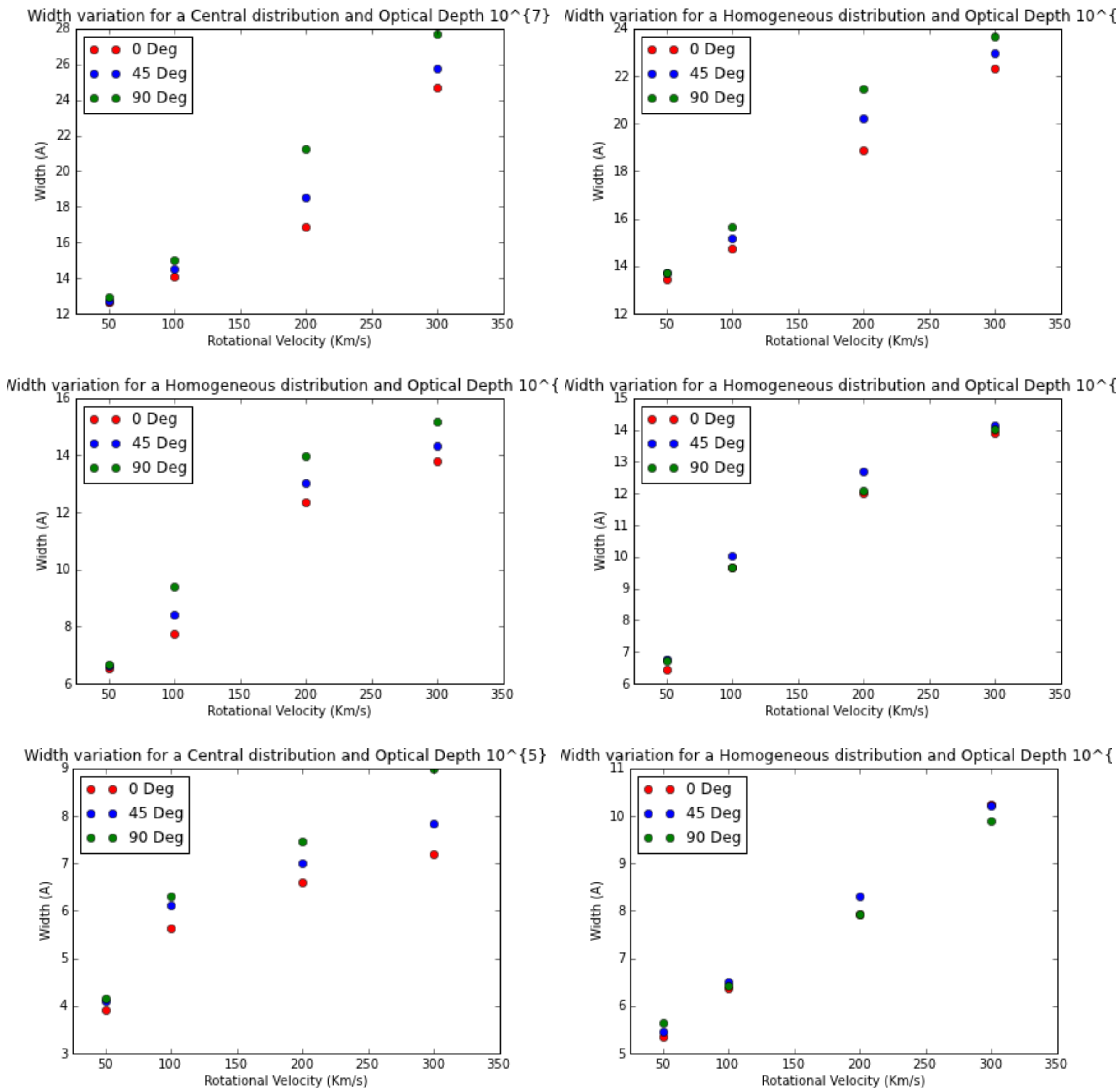

Figure 4. Width of the lyman-alpha line for all the models.

Velocity (km/s)	Maximum 1 position	Maximum 2 position
50	-7.46286	6.53714
100	-7.53357	6.96643
200	-8.17453	7.32547
300	-6.81487	6.18513

Table 3. Optical Depth $\tau = 10^6$, Central Distribution

Velocity(Km/s)	Maximum 1 position	Maximum 2 position
50	-4.33708	3.66292
100	-4.27326	3.72674
200	-3.7737	3.7263
300	-3.84903	4.15097

Table 4. Optical Depth $\tau = 10^5$, Central distribution

Escape fraction

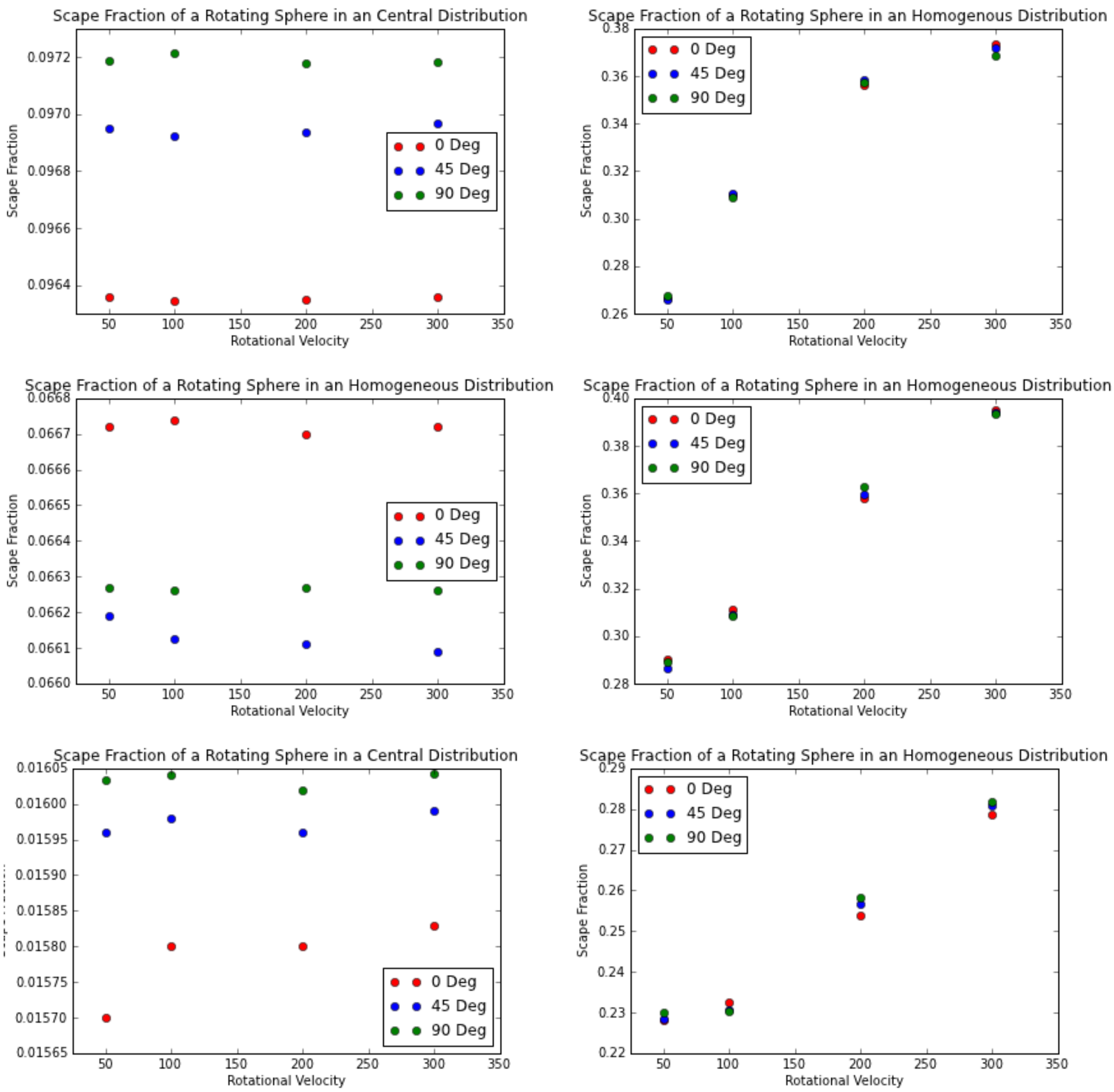

Figure 6. Escape fraction for all the models. Left panels show the central distribution, while right panels show the homogeneous distribution

Velocity(Km/s)	FWHM	θ
50	12.62	0^o
50	12.72	45^o
50	12.93	90^o
100	14.07	0^o
100	14.48	45^o
100	15.00	90^o
200	16.90	0^o
200	18.51	45^o
200	21.24	90^o
300	24.69*	0^o
300	25.79*	45^o
300	27.73*	90^o

Table 5. Lines Widhts for a Central Distribution and $\tau = 10^7$

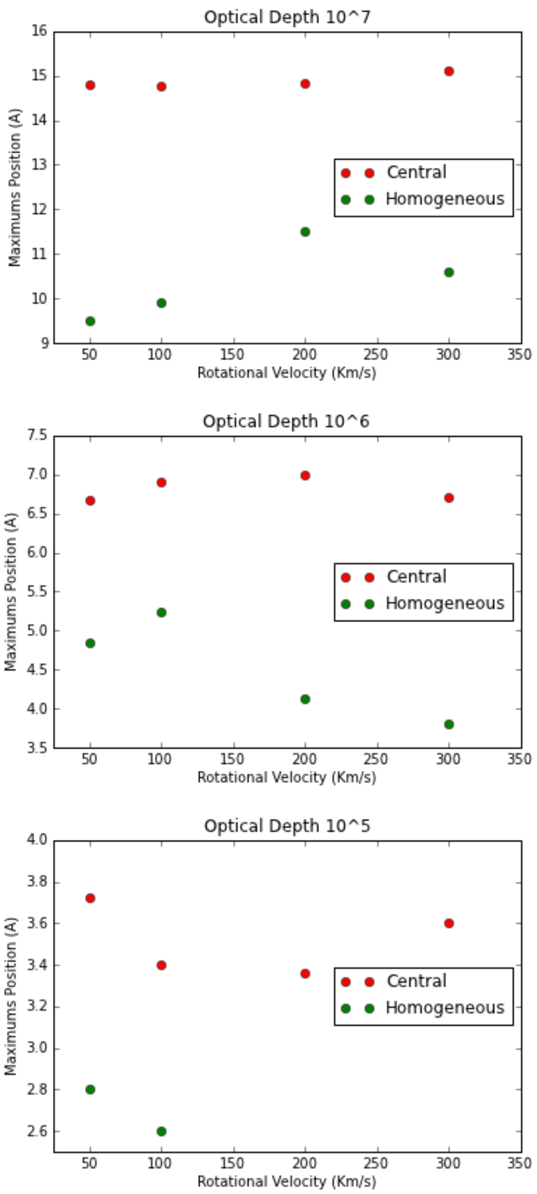

Figure 3. Width of the lyman-alpha line for all the models.

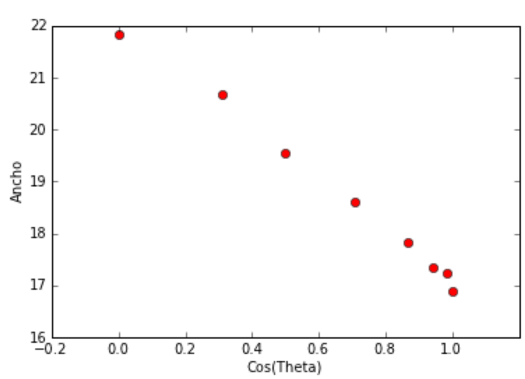

Figure 5. Width variation in function of theta

[H]

Model	Velocity (km/s)	θ	Dust $\sum(s)$	$\sum(s)$
Homogeneous	50	0^o	13293.06	49939.53
Homogeneous	50	45^o	13291.04	50001.59
Homogeneous	50	90^o	13348.76	49922.73
Homogeneous	100	0^o	15527.69	50114.11
Homogeneous	100	45^o	15511.56	49967.17
Homogeneous	100	90^o	15401.71	49833.65
Homogeneous	200	0^o	17830.85	50078.69
Homogeneous	200	45^o	17932.87	50064.42
Homogeneous	200	90^o	17830.85	49931.748
Homogeneous	300	0^o	18687.33	50048.33
Homogeneous	300	45^o	18572.12	49922.67
Homogeneous	300	90^o	18421.79	49979.37

Table 6. Escape fraction for a Homogeneous Distribution and optical depth 10^5.

Model	Velocity (km/s)	θ	Dust $\sum(s)$	$\sum(s)$
Central	50	0^o	4809.881	49917.069
Central	50	45^o	4829.21	49811.79
Central	50	90^o	4845.108	49853.039
Central	100	0^o	4809.665	49921.30
Central	100	45^o	4828.65	49820.13
Central	100	90^o	4846.45	49854.0
Central	200	0^o	4809.63	49917.64
Central	200	45^o	4829.25	49818.49
Central	200	90^o	4844.89	49856.66
Central	300	0^o	4810.56	49922.98
Central	300	45^o	4831.16	49823.33
Central	300	90^o	4845.33	49858.48

Table 7. Escape fraction for the central Distribution and optical depth 10^5.